

# Minimal Architecture Zinc-Bromine Battery for Low Cost Electrochemical Energy Storage

Shaurjo Biswas<sup>1</sup>, Aoi Senju<sup>2</sup>, Robert Mohr<sup>1</sup>, Thomas Hodson<sup>1</sup>, Nivetha Karthikeyan<sup>1</sup>, Kevin. W. Knehr<sup>1</sup>, Andrew G. Hsieh<sup>1</sup>, Xiaofeng Yang<sup>2</sup>, Bruce Koel<sup>2</sup>, Daniel A. Steingart<sup>1,2,\*</sup>

<sup>1</sup>*Department of Mechanical and Aerospace Engineering & the Andlinger Center for Energy and The Environment, Princeton University, NJ, 08544, USA*

<sup>2</sup>*Department of Chemical and Biological Engineering, Princeton University, NJ, 08544, USA*

*Corresponding Author: \*email: steingart@princeton.edu, Ph.: (609) 258-1257, Address: Room 213 ACEE, 86 Olden St., Princeton, NJ, USA. 08544-5263*

Keywords: Energy storage, zinc-bromine cell, membrane-free, non-flowing battery, carbon foam electrode, low cost, aqueous electrolyte

## Supplementary Information

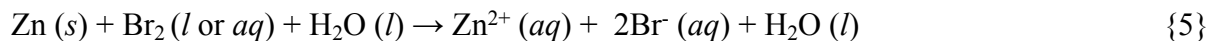
### Reactions in the Cell

The ZnBr<sub>2</sub> cell operates in acidic conditions. Some H<sub>2</sub> (g) is formed due to corrosion of the Zn metal in acid, and some Zn (s) is consumed by the dissolved Br<sub>2</sub> (aq) species. In an ideal case the generated H<sub>2</sub> (g) would recombine with the Br<sub>2</sub> as well.

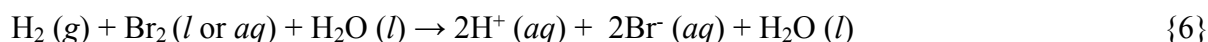
The desired primary reactions are:



with the potential side reactions of:



and finally, the beneficial recovery of H<sub>2</sub> (g) via:



Thus, taken together, without irreversible consumption of the electrode materials, a reaction scheme can be envisioned such that any phenomena related to non-unity coulombic efficiency can be reversed.

### Carbon Foam Electrode (CFE) Preparation

The foams are prepared by the following method: A 30:70 weight ratio of graphite and carbon black (total weight = 0.9 g) is mixed in a 5 wt% solution of polyvinylidene difluoride (PVDF) in N-Methyl-2-pyrrolidone (NMP) to create a carbon slurry. PVDF is used as the binder (1:9 PVDF:carbon weight ratio) and is one of the few materials resistant to liquid bromine corrosion. Carbon fiber leads are inserted in the slurry to ensure good electrical contact, which is then poured into a mold with retractable pistons (3D printed in a FormLabs Form 1+) and compressed

using a hydraulic press to  $\sim 1$  psig to improve the carbon compaction. The mold is then placed in a vacuum oven and baked for 12 hr at  $90^\circ\text{C}$ , evaporating the NMP and leaving behind a porous but rigid carbon foam. Porosities of over 80% with a mean pore size of  $\sim 400$  nm have been achieved. The foam porosity and pore size distribution may be tuned by altering the slurry composition, hydraulic pressure, baking time, and baking temperature, among other processes. The porosity and pore size distribution were measured by mercury porosimetry and SEM. The three CFE sizes discussed in **Fig. 3b** are prepared in the same way, the only difference being their length of 10, 20, and 29 mm.

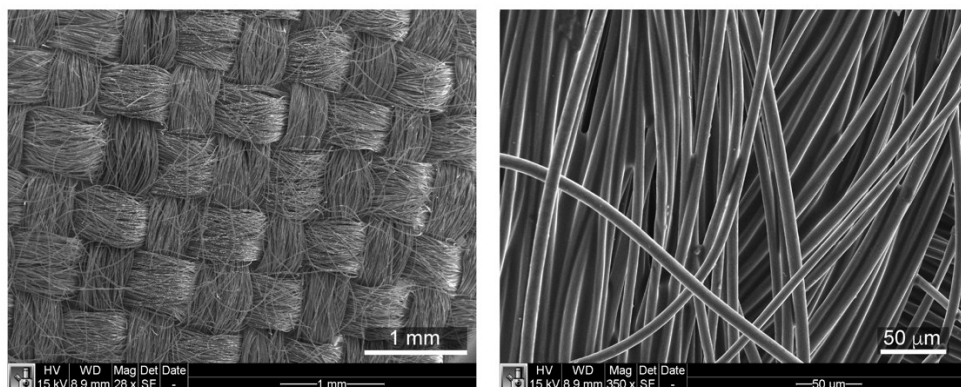


**Figure S1:** SEM images of the carbon cloth used as the negative electrode.

### Electrode Characterization

The carbon cloth negative electrode is a standard fuel cell electrode - graphitized spun yarn woven fabric with a fiber diameter of  $6\ \mu\text{m}$  and yarn width of  $0.4\ \text{mm}$  with a count of  $17 \times 17 / \text{cm}^2$ . The area of each cloth face exposed to  $\text{ZnBr}_2$  electrolyte is  $1\ \text{cm}^2$  through all the experiments. Zinc is observed to grow only on the outer face of the carbon cloth, as shown in **Fig. 1c**. Preliminary SEM images (**Figure S1**) suggest that Zn is not deposited within the yarn. Assuming this to be the case the surface area available for zinc growth is  $\sim 1.4\ \text{cm}^2$ . If the fiber diameter was to be increased and the weave was coarser, the surface area available for zinc deposition would be higher, current density would be lower, and the initial growth front would be more uniform. However, a coarser weave and higher fiber diameter would result in lower conductivity of the electrode resulting in higher IR losses and, thus, lower coulombic and energy

efficiency. In the MA-ZBB, the carbon cloth negative electrode is less significant than the CFE in terms of limiting the efficiencies of the system.

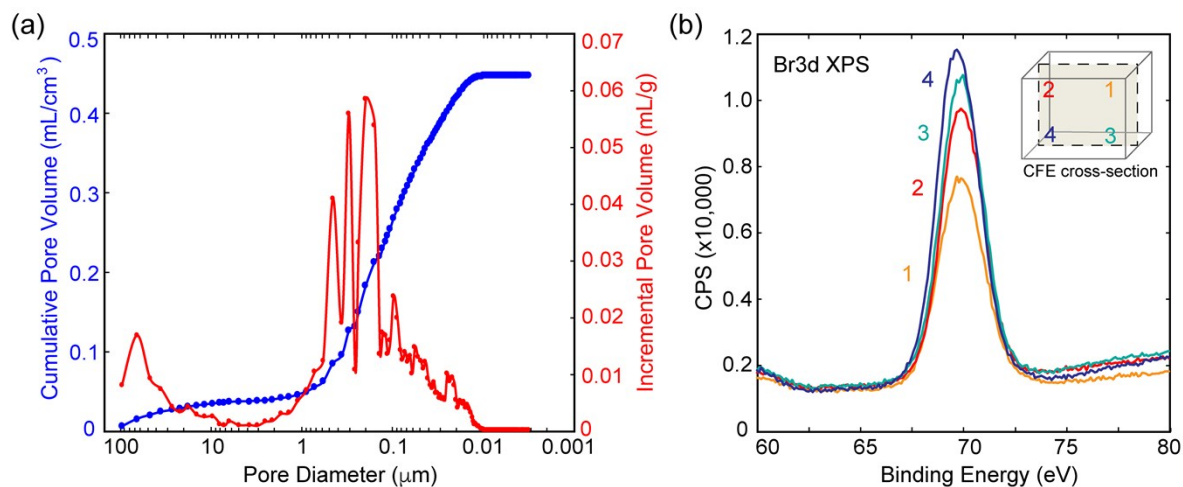


**Figure S2:** (a) Mercury porosimetry data of CFE used as the negative electrode in MA-ZBB cells. (b) XPS data from 4 locations in the cross-section of a CFE used in a cell cycled 50 times at 20 mA 2 hr CC.

The self-discharge of the cell, and the coulombic efficiency of the MA-ZBB system is determined primarily from the volume of  $\text{Br}_2(l)$  in the electrolyte during charging.  $\text{Br}_2(l)$  (and poly-bromide ions,  $\text{Br}_3^-$ ) diffuse to the negative electrode through the aqueous electrolyte and corrode the plated zinc during charging, in the absence of a separator. The CFE used as the positive electrode in the cell can store the generated  $\text{Br}_2(l)$  within its pores and prevent self-discharge. The CFE used in the experiments reported here have been characterized by SEM, mercury porosimetry, XPS, and color-concentration tracking. The SEM image in **Fig. 1e** shows some large cavities on the CFE surface, but the mean pore diameter measured by porosimetry is  $0.58 \mu\text{m}$  and total pore volume is  $0.461 \text{ ml/cm}^3$ , shown in **Fig. S2a**. However, color-concentration tracking indicates that only  $0.024 \text{ ml}$  of  $\text{Br}_2(l)$  generated is stored in the  $1 \text{ cm}^3$  CFE, shown in **Fig. 2b**: when onset of color increase is detected at point *1*. We hypothesize that the generated  $\text{Br}_2(l)$  is only stored in the pores of the CFE and cannot penetrate into its core. This is further verified by studying the XPS data collected from points *1-4* within the CFE, shown in **Fig. S2b**, where the counts of  $\text{Br}_2$  increases from top to bottom and from inside to outside. As shown in **Fig. 3b**, the volume of  $\text{Br}_2(l)$  that can be stored in the CFE scales with the

geometric volume of the foam. Further increase in the maximum  $\text{Br}_2(l)$  storage within the CFE, and thus maximum utilized cell capacity, can be obtained by modifying the CFE geometry. For example, if the CFE is a hollow cube (CFE-shell), it could potentially store larger volumes of  $\text{Br}_2(l)$  within it, thus improving the operating capacity of the battery.

### Apparatus construction

Cell design is critical to achieving the highest performance of the MA-ZBB battery. The components of the cell are: 1) borosilicate glass holder (inner volume of  $1 \times 3 \times 5 \text{ cm}^3$ ), 2) carbon foam electrode ( $1 \text{ cm}^3$  volume, 1 g weight), 3) carbon cloth electrode ( $1 \text{ cm}^2$  exposed area, rest is sealed with PTFE to prevent wicking), 4) aqueous  $\text{ZnBr}_2$  electrolyte (2M solution), and 5) carbon fiber leads (any exposed surface outside the CFE is coated with PTFE to prevent wicking). The MA-ZBB battery is non-flowing, or more accurately non-forced-flowing design, due to the absence of pumps. However, there is considerable species transport within the cell.

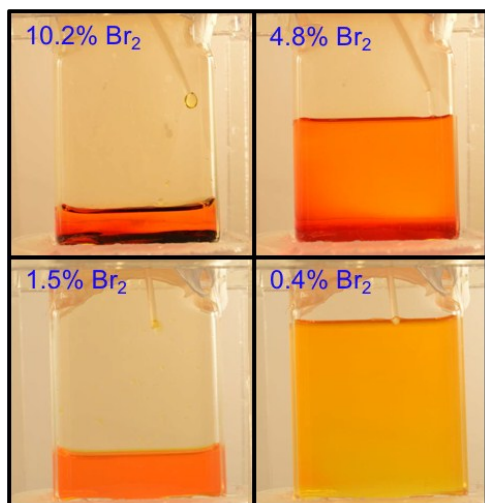


**Figure S3:** Sample images of solutions with  $\text{Br}_2$  volume % in 2 M  $\text{ZnBr}_2$  solution.

### Bromine color-concentration calibration and tracking

A cell with 5 mL  $\text{Br}_2(l)$  (10.2% by volume) in DI water solution is placed in a light box illuminated with two white light sources. The clear glass cell holder enables direct imaging of the system. A 0.05 mL of 2M  $\text{ZnBr}_2$  salt solution is added to the cell using a calibrated syringe pump

every 3 min and stirred to obtain uniform concentration profiles. The cell is placed in a closed light box with two white light sources (50W, 6,000K color temperature) to maintain a uniform background color. Images are captured every 10 s using a Nikon D300 SLR camera with manual white light balance, aperture, shutter speed and ISO set and maintained across all experiments. Four sample calibration cells are shown in **Supplementary Information Figure S3** with  $\text{Br}_2(l)$  volumetric concentrations in solution of 10.2%, 4.8%, 1.5%, and 0.4%, respectively. The calibration data relating the  $\text{Br}_2(l)$  volume concentration to CIE  $X$  and  $Y$  color coordinates are presented in **Supplementary Information Figure S4**. The CIE  $X$  and  $Y$  color coordinates at each concentration is obtained by averaging the RGB pixel values of a fixed 5 mm x 12 mm frame of the images obtained at each volumetric concentrations of the  $\text{Br}_2(l)$  solution, and converting the RGB values to standard 1931 CIE  $X$  and  $Y$  coordinate space. Third order polynomial fits (dashed lines) are used to correlate the color of the solution to its concentration.

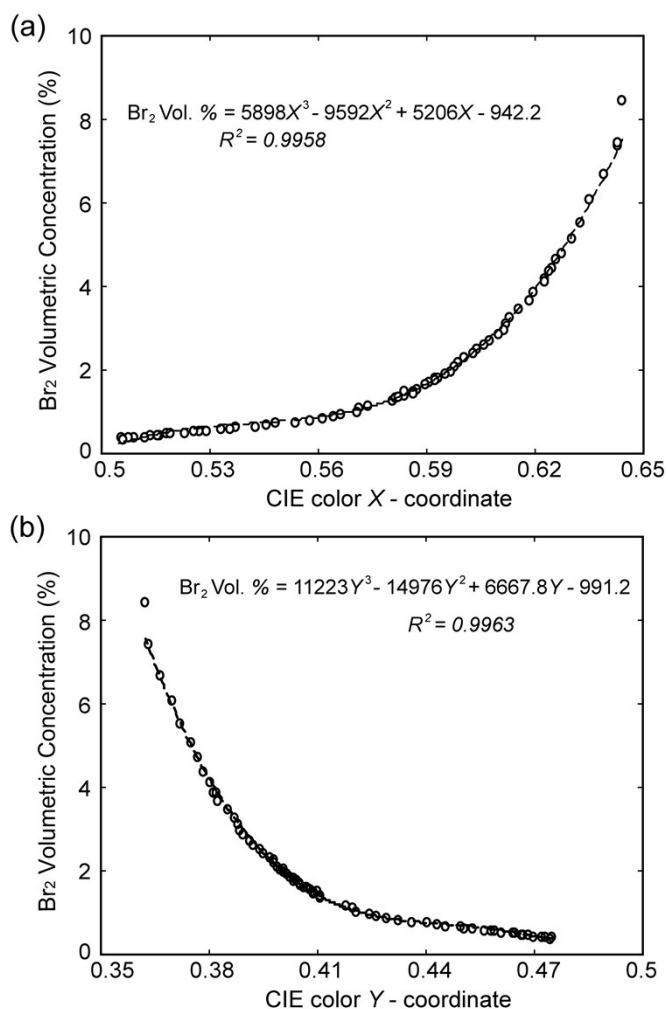


**Figure S4:** Calibration data CIE 1931  $X$  and  $Y$  coordinates related to the  $\text{Br}_2$  volume % in 2M  $\text{ZnBr}_2$  solution in (a) and (b). The third-order polynomial fit (dashed line) is used for extracting the  $\text{Br}_2$  volumetric concentration in MA-ZBB cells during operation using the optical tracking method.

Optical tracking on MA-ZBB cells during battery operations is performed by using the same light box and camera set up. The RGB values at any point in the image is extracted and converted to CIE  $X$  &  $Y$  coordinates, which is then related to  $\text{Br}_2(l)$  volumetric concentration at that point using the calibration fit, described above. This enables the comparison of different cells and architectures, as well as the tracking and analysis of bromine and zinc transport during operation, as depicted in **Fig. 2**.

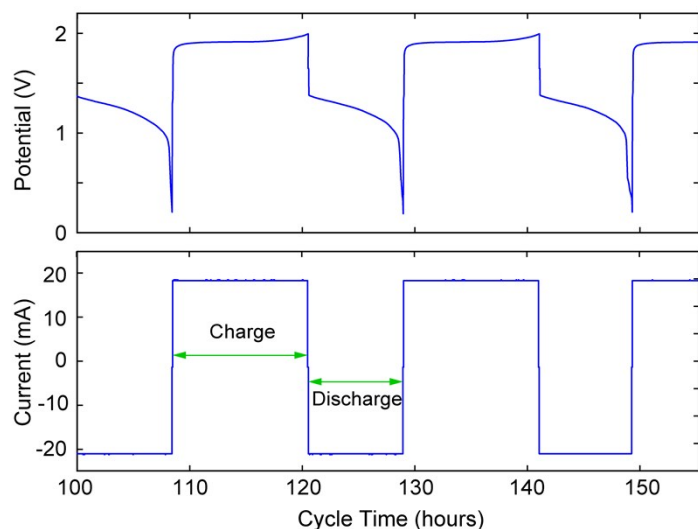


**Figure S5:** Current voltage characteristics of an MA-ZBB cell that is charged and discharged at 20 mA to 2 V and 0.2 V, respectively. The charge and discharge times steps (shown with green arrows) are ~12 hr and ~8.4 hr, respectively. The maximum charge capacity recorded here is ~240 mAh.

### Electrochemical testing

Leads from the MA-ZBB electrodes are connected to a constant current supply source (Keithley 2401) to monitor the cell potential and resistance during galvanostatic cycling. Multi-cell cycling is done with a MTI Corp. 8-channel battery analyzer.

For the analysis shown in **Fig. 3a**, cell voltage, capacity, coulombic and energy efficiencies are recorded for 10 cycles at each discharge current. The discharge voltage cut-off limit is 0.2 V in all experiments. Three identical cells (2M ZnBr<sub>2</sub> solution, 30:70 weight ratio CFE, in identical glass holders) are charged for 2 hours at 20 mA (imposed charge capacity of 40 mAh, based on color tracking results of **Fig. 2**) and discharged at 80 mA. The efficiencies are averaged across the 10 cycles of each cell. The average efficiencies with *y-axis* error bars (representing the best and worst efficiencies recorded) are plotted against 2C rate in **Fig. 3a**. The process is then repeated for discharge currents of 0, 1, 3, 5, 10, 20, 30, and 40 mA and cell efficiencies are plotted in the figure.

The lifetime study shown in **Fig. 4a** is performed in a separate set of experiments. A MA-ZBB cell is subjected to a total of 500 cycles at various charge-discharge currents. In this galvanostatic cycling experiment, the cell is charged for 2 hr at a given current and discharged at the same current with a discharge voltage limit of 0.2 V. The cell is charged and discharged for 100 cycles each at currents of 5, 50, 40, 20 mA, and again 5 mA in that order, using a fixed 2-hour charge step. The coulombic and energy efficiencies recorded are plotted against cycle life in **Fig. 4a**. **Fig. 4b** shows 1,000+ cycles of the cell. The cell was cycled by charging at 20 mA for 2 hours and discharging at 20 mA until a discharge voltage limit of 0.2 V.

Each cell (2M ZnBr<sub>2</sub> solution, 30:70 weight ratio CFE) can be charged for 12 hours at 20 mA before the cell potential hits the cutoff of 2.0 V. The maximum available capacity of this cell design is experimentally determined to be 240 mAh. A cell is set up with a charge cutoff voltage of 2.0 V and discharge cutoff voltage of 0.2 V. When the cell is cycled at 20 mA, the voltage limit is reached in 12 hr during charging and 8.4 hrs during discharge. The current - voltage characteristics of this cell is shown in **Supplementary Information Figure S5**. The gradual increase of measured potential toward the end of each charge step is due to the depletion of Br<sup>-</sup> ions in solution in the vicinity of the CFE. Hence, we claim that the maximum charge capacity of this MA-ZBB cell is ~240 mAh. Better cell design will result in improved capacity utilization.

### **Variations of electrolyte composition**

Another point worth noting is that the MA-ZBB cell has no additives in the electrolyte. The pH of the solution is 4.57. The pH of the electrolyte was adjusted to values of 1.61, 2.22, 3.18, and

4.57 by adding HBr, and MA-ZBB cells were charged at 20 mA for 2 hr and discharged at 20 mA to 0.2 V. As shown in **Supplementary Information Figure S6**, the coulombic and energy efficiencies increases as pH decreases. This improved performance could be a result of either a shift in reaction equilibrium or an increase in ionic conductivity. When the pH is  $< 1.5$ , the plated zinc is etched away by the acid, leading to loss of cell performance. This is currently a study in progress.

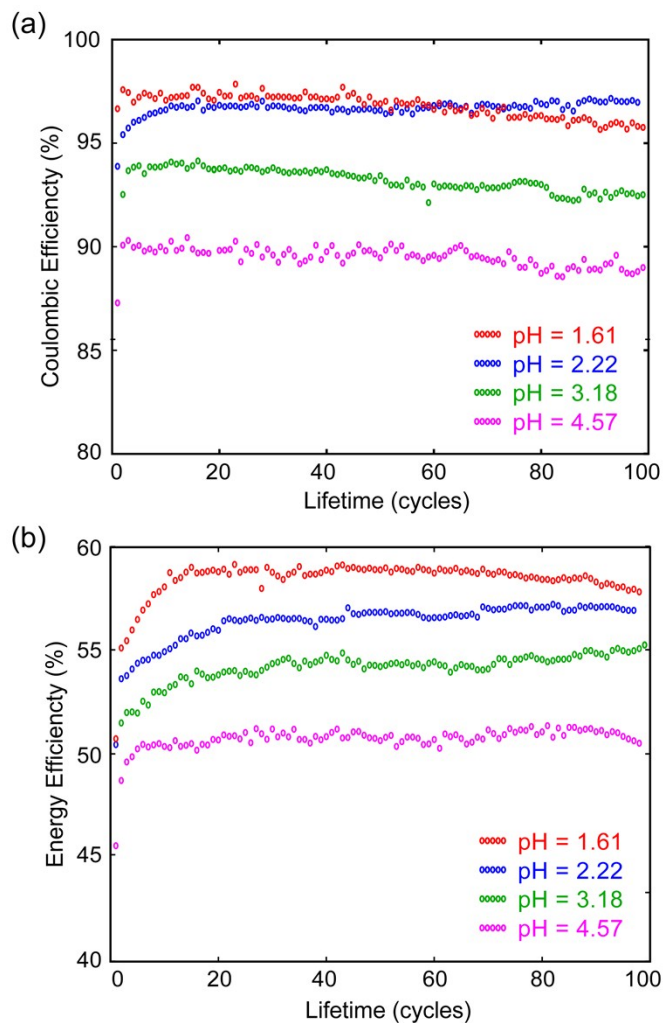


**Figure S6:** (a) Coulombic and (b) energy efficiencies of MA-ZBB cells with HBr added resulting in pH = 1.61, 2.22, 3.18, and 4.57. The cells are charged and discharged at 20 mA with a fixed 2 hr charge step and a 0.2 V lower potential limit for 100 cycles.

## Hydrogen Generation

Since the cell is operated in a slightly acidic solution ( $\text{pH} = 4.57$ ), there is a small amount of  $\text{H}_2(\text{g})$  generation on the Zn electrode. The hydrogen gas generated during the first five cycles of a cell was determined by monitoring the pressure in the headspace. A special cell was fabricated by sealing a 3-D printed lid to the glass holder with epoxy. Pressure changes were monitored using a board mount pressure sensor (Honeywell, SSC D RR N 015 PD A A 5). The cell was cycled at 20 mA with a 2 hr charge followed by a discharge to 0.2 V. A 120 s rest period was included between all charge/discharge steps. **Supplementary Information Figure S7** shows the pressure and voltage of the cell. The pressure rise during charge can be attributed to the electrochemical generation of  $\text{H}_2(\text{g})$ , while the pressure rise during discharge results from  $\text{H}_2(\text{g})$  produced by the corrosion of Zn metal. The delay in pressure rise at the start of cycling can be attributed to uptake of soluble  $\text{H}_2(\text{g})$  in the electrolyte.

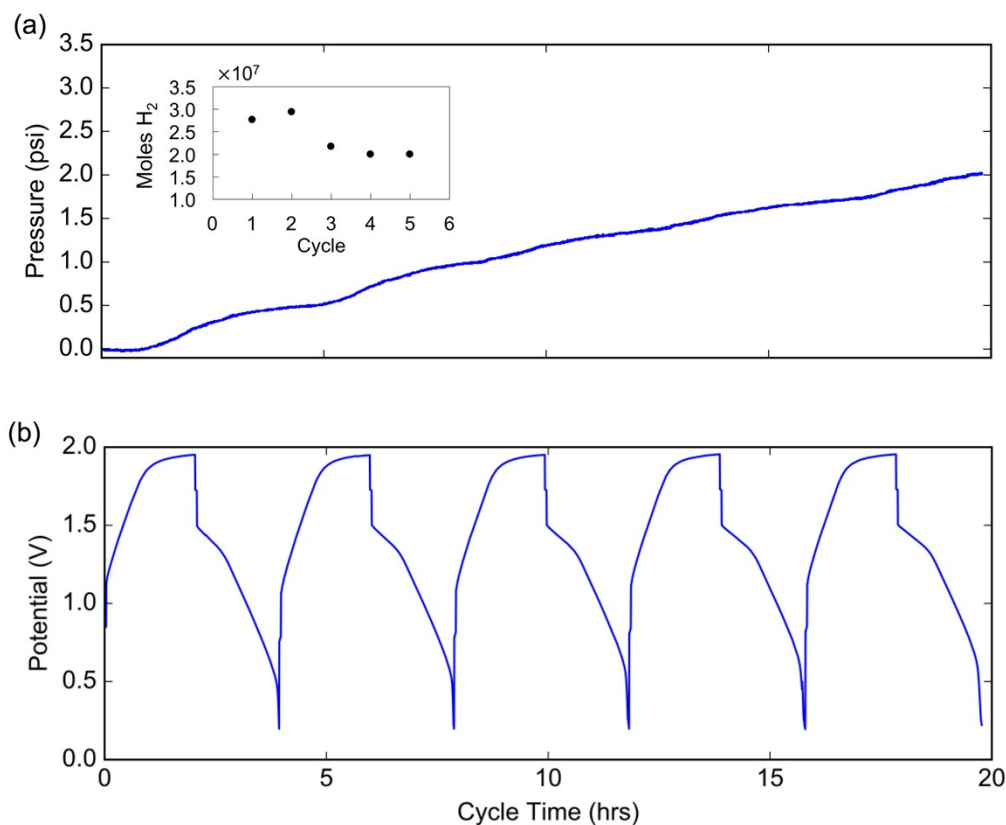


**Figure S7:** Characterization of hydrogen generation. **(a)** Pressure and **(b)** voltage response of a sealed cell during cycling at 20 mA with 120 s rest periods between charge and discharge steps. Cell was charged for 2 hours and discharged to a cutoff of 0.2 V. **Inset in (a):** Moles of hydrogen generated per cycle, which was calculated from the change in pressure over a single charge/discharge cycle.

The moles of hydrogen generated during cycling were determined assuming *i*) an ideal gas and *ii*) the electrolyte was fully saturated with  $\text{H}_2(\text{g})$  at its respective partial pressure. The results (see inset in **Figure S7**) indicate that  $\sim 2.0 \times 10^{-7}$  moles of  $\text{H}_2(\text{g})$  are generated per cycle (or  $<0.03\%$  of the total capacity). Note, this represents a worse case scenario due to a large headspace in the cell to account for measurement equipment. We anticipate the rate of  $\text{H}_2(\text{g})$  generation to decline with a smaller headspace (and over longer cycling) due to increases in soluble  $\text{H}_2$  in the electrolyte. In fact, a decrease in the rate of  $\text{H}_2$  generation is already observed over the first five cycles (inset in **Figure S7**).

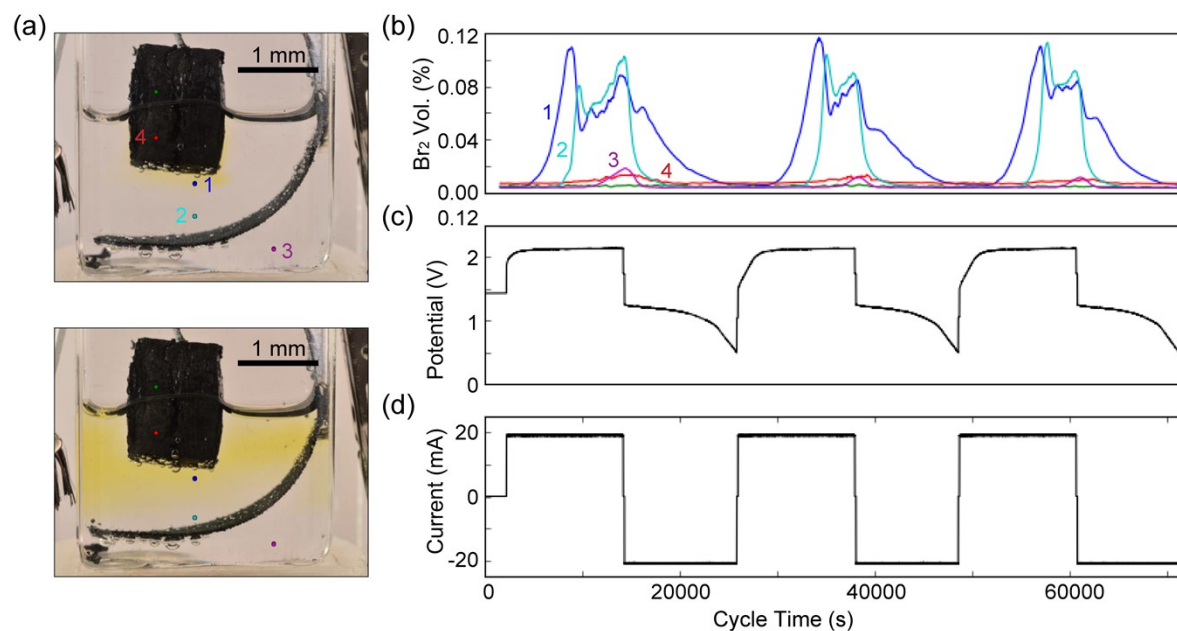


**Figure S8:** As a strategy to recapture any generated  $\text{H}_2(\text{g})$ , an inverted MA-ZBB cell was designed. **(a)** Photographs of the inverted cell design, showing the points where **(b)** color-concentration tracking is monitored during operation. **(c,d)** The cell is charged and discharged at 20 mA with a 3.2 hours charge step.  $\text{H}_2(\text{g})$  that is generated at the negative current collector carbon cloth (bottom) reacts with the  $\text{Br}_2(\text{aq/l})$  that is generated at the top of the cell around the CFE.

To counter the  $\text{H}_2(\text{g})$  problem for larger systems in the future, we submit a new cell design, shown in **Supplementary Information Figure S8**. Here, the CFE is placed on top of the cell,

while the negative carbon cloth electrode is at the bottom. When  $H_2(g)$  is generated at the bottom of the cell and bubbles upward, the  $Br_2(l/aq)$  present around the CFE on top of cell could potentially be made to react (in the presence of UV light/heat) with  $H_2(g)$  and redissolve it into solution as  $HBr(l)$ , thus recapturing any potential losses.

### Cost analysis

The costs reported for the lab-scale MA-ZBB system are estimated based on current market prices for materials. The current and projected system costs of \$176/kWh and \$94/kWh, respectively, are only for the bill of materials and does not include transportation, overhead, or labor costs. The LCOES for this system is defined as \$/kWh over its lifetime (number of cycles) and energy efficiency. The LCOES of the projected MA-ZBB is calculated as \$94/kWh / 0.6 energy efficiency / 1,000 cycles, which is \$0.159/kWh/cycle. The range of projected LCOES for the same design is obtained by changing 1000 cycles to 8,000 - 10,000 cycles, keeping the \$/kWh and the energy efficiency the same. The LCOES breakdown of other commonly used, commercially available battery systems (traditional lead acid, lithium ion, sodium sulphide, vanadium and Zn-Br redox flow batteries (RFB)) is calculated from the data provided in the **Supplementary Information Table S1**. The range of the LCOES is shown as the ovals in **Fig. 5** and the band within the oval represents the average of the most commonly-reported \$/kWh/energy efficiency/cycle life values for these systems.

Technology	\$/kWh range	\$/kWh avg.	Cycle range	Cycle avg.	EE range (%)	EE Avg. (%)	Avg. LCOES (\$/kWh/cyc/%)
C-Pb Acid	330 - 480	405	400-800	600	75-90	82.5	0.81
Li-ion	680-900	790	1200-4000	1500	87-94	90	0.58
NaS	350-400	375	800-1500	1200	70-80	75	0.42
V RFB	370-550	460	5000-12000	10000	65-75	70	0.065
Zn-Br RFB	280-400	340	6000-10000	8000	60-70	65	0.052
<b>MA-ZBB (projected)</b>	50-100	93.6	7000-10000	9000	60-70	60	0.017

**Table S1:** Cost, cycle life, and energy efficiency of EES technologies.<sup>13,24,25</sup>